# The *Saccharomyces cerevisiae* RNase Mitochondrial RNA Processing Is Critical for Cell Cycle Progression at the End of Mitosis

**Ti Cai, Jason Aulds, Tina Gill, Michael Cerio and Mark E. Schmitt**[1]

*Department of Biochemistry and Molecular Biology, State University of New York Upstate Medical University, Syracuse, New York 13210*

Manuscript received December 12, 2001
Accepted for publication April 25, 2002

ABSTRACT

We have identified a cell cycle delay in *Saccharomyces cerevisiae* RNase MRP mutants. Mutants delay with large budded cells, dumbbell-shaped nuclei, and extended spindles characteristic of "exit from mitosis" mutants. In accord with this, a RNase MRP mutation can be suppressed by overexpressing the polo-like kinase *CDC5* or by deleting the B-type cyclin *CLB1*, without restoring the MRP-dependent rRNA-processing step. In addition, we identified a series of genetic interactions between RNase MRP mutations and mutations in *CDC5*, *CDC14*, *CDC15*, *CLB2*, and *CLB5*. As in most "exit from mitosis" mutants, levels of the Clb2 cyclin were increased. The buildup of Clb2 protein is not the result of a defect in the release of the Cdc14 phosphatase from the nucleolus, but rather the result of an increase in *CLB2* mRNA levels. These results indicate a clear role of RNase MRP in cell cycle progression at the end of mitosis. Conservation of this function in humans may explain many of the pleiotropic phenotypes of cartilage hair hypoplasia.

RIBONUCLEASE mitochondrial RNA processing (RNase MRP) is a ribonucleoprotein endoribonuclease that cleaves an RNA sequence in a site-specific manner (Chang and Clayton 1987). RNase MRP was initially isolated from mammalian mitochondria; however, cellular fractionation and immunolocalization experiments have revealed that the majority of the complex is localized to the nucleus of mammalian cells (Reimer *et al.* 1988). The enzyme has been remarkably conserved from yeast to humans in both the RNA and protein components (Schmitt and Clayton 1992; Lygerou *et al.* 1996; van Eenennaam *et al.* 2000). In the yeast *Saccharomyces cerevisiae*, a role for RNase MRP in nucleolar processing of rRNA has been found (Schmitt and Clayton 1993; Chu *et al.* 1994; Henry *et al.* 1994). Mutations in the RNA component of the human RNase MRP have been shown to be the cause of the genetic disease cartilage hair hypoplasia (CHH; Ridanpää *et al.* 2001). This disease is characterized by short stature, brittle and sparse hair, and immunodeficiency (Mäkitie *et al.* 1995; Clayton 2001).

The gene for the *S. cerevisiae* MRP RNA is called *NME1* for *n*uclear *m*itochondrial *e*ndonuclease 1 (Schmitt and Clayton 1992). In addition, at least nine yeast proteins associated with the MRP RNA *in vivo* have been identified. Eight of these proteins are shared with the ribonucleoprotein endoribonuclease RNases P (Lygerou *et al.* 1994; Chu *et al.* 1997; Dichtl and Tollervey 1997; Stolc and Altman 1997; Chamberlain *et al.* 1998). One protein encoded by the *SNM1* gene encodes an RNA-binding protein that is associated only with the RNase MRP RNA and not the RNase P RNA (Schmitt and Clayton 1994).

All of the components of RNase MRP are essential for the viability of yeast. Mutations in the yeast RNase MRP components lead to a defect in 5.8S-rRNA processing, specifically at the $A_3$ site in the pre-rRNA (Schmitt and Clayton 1993; Chu *et al.* 1994; Henry *et al.* 1994). Removal of the $A_3$ processing site and loss of mitochondrial DNA are not lethal in yeast, indicating that there is an unknown essential function for RNase MRP (Henry *et al.* 1994; Venema and Tollervey 1999). In support of this idea, mutations in the *SNM1* gene can lead to defects in plasmid stability (Cai *et al.* 1999). In *Schizosaccharomyces pombe*, a mutation in the MRP RNA was found to lead to a defect in septation (Paluh and Clayton 1996). The cause of the phenotypes in these mutants was not determined.

We report here the identification of a specific cell division cycle delay in RNase MRP mutants. Cells accumulate late in the mitotic cycle with large budded cells, dumbbell-shaped nuclei, and extended spindles, identical to that seen with previously described exit from mitosis mutants (EFM; Surana *et al.* 1993). A series of genetic interactions were identified between mutations in RNase MRP components and known EFM genes. Western analysis of the mitotic cyclin Clb2 showed accumulation of Clb2 protein as is the case in most EFM mutants. These observations suggest an entirely novel role for RNase MRP in control of the cell cycle and potentially identify its essential function. In addition, the cell cycle delay lends insights as to the cause of the pleotropic phenotypes seen in CHH (Mäkitie *et al.* 1995).

[1]*Corresponding author:* Department of Biochemistry and Molecular Biology, State University of New York Upstate Medical University, 750 E. Adams St., Syracuse, NY 13210. E-mail:schmittm@upstate.edu

## MATERIALS AND METHODS

**Strains and media:** Yeast media and genetic manipulations have been described (Cai *et al.* 1999). Basic molecular biology techniques were performed as described (Sambrook *et al.* 1989). The genotypes of all yeast strains used are given in Table 1.

**Construction of the yeast strain YMC6:** YMC6 expresses three tagged subunits of the RNase MRP enzyme simultaneously: *Snm1:GFP:6HIS*, *Pop3:GFP*, and *Pop4:3×HA*. To construct this strain the *POP3* gene was deleted in the strain MES101 and marked with the *HIS3* gene (Longtine *et al.* 1998) to create the strain YGB22 (see Table 1). This strain was transformed with the plasmid pTC143 (pRS315 carrying the *POP3* gene) to generate the strain YGB24 and was subsequently sporulated to generate the strain YGB24-38A. YL323 was transformed with the plasmid pSC93 (kind gift of L. Lindahl, University of Maryland; Chu *et al.* 1997) and subsequently sporulated to generate the strain YGB26-14D. YGB26-14D was mated to YGB24-38A to create the diploid strain YGB28 and the two plasmids were allowed to be lost. This strain was transformed with the plasmid pGAB116 (contains both a *GFP:POP3* fusion gene and a *POP4:3XHA* gene; Chu *et al.* 1997). The resulting strain, YGB29, was sporulated and the double *pop3* and *pop4* mutant YGB29-4A was chosen for subsequent use. The strain, THR200, was transformed with the plasmid pGAB119 (*SNM1:GFP:6His*, *LEU2*; Cai *et al.* 1999). The resultant strain YGB30 was crossed to YGB29-4A and the diploid, MES250, was sporulated. A strain with chromosomal deletions of *snm1*, *pop3*, and *pop4* was selected and named YMC6.

**Construction of the *CDC14-GFP* fusion:** PCR-targeted gene modification was performed as described (Longtine *et al.* 1998). Primers were used to amplify the *CDC14* gene and the pFA6a-GFP(S65T)-kanMX6 cassette placing the green fluorescent protein (GFP) tag exactly before the *CDC14* termination codon. The final PCR product was purified and transformed into the strain MES117. The transformants were plated on YPD-G418 plates to select for the fusion. The *CDC14-GFP* construct was verified by PCR and fluorescence microscopy. RNase MRP RNA mutants were shuffled into the resulting strain YTC240 as previously described (Shadel *et al.* 2000).

**Immunofluorescence microscopy:** Cells were prepared for immunofluorescence as previously described (Pringle *et al.* 1991). Rat monoclonal antitubulin antibody, YOL1/34, and Cy3 conjugated rabbit anti-rat secondary antibody were obtained from Accurate Chemical (Westbury, NY). Cells were viewed using a Zeiss Axioskop microscope equipped with epifluorescent and Nomarski optics and a Zeiss Plan-Apochromat ×100 objective. Images were captured in real time using a Diagnostics Instruments Spot Camera 2 directly linked to an Apple PowerMac G3 computer.

**Plasmid segregation assay:** Plasmid segregation assays were carried out as previously described (Cai *et al.* 1999), using the yeast strains MES111-140 as a wild-type control and MES111-P6 as the experimental.

**Identification of high-copy suppressors of the *snm1-172* mutation:** The yeast strain YTC150-172 carrying the *snm1-172* mutation (T189G; G190C [Cys64Ala] in the *SNM1* gene; Cai *et al.* 1999) was transformed with a yeast, *URA3*, 2μ genomic library (Carlson and Botstein 1982) and plated onto Ura$^-$ media at 24°. Ten thousand transformants were replicated to synthetic complete dextrose media (SCD; Shadel *et al.* 2000) at 37°. Colonies growing at the nonpermissive temperature were picked and retested. Those transformants that continued to grow at 37° on SCD plates, but failed to grow at 37° on SCD plates with 5-fluoroorotic acid, were classified as plasmid-linked suppressors. Yeast 2μ plasmids that conferred 37° growth were rescued from yeast into *Escherichia coli* (Sikorski and Boeke 1991) and then retested for suppression in the original *snm1-172* strain.

**Cell arrest experiments:** Yeast strains were grown to $10^6$ cells/ml at 25° in SCD, arrested in hydroxyurea (15 mg/ml) or nocodazole (20 μg/ml) for 3 hr, and then shifted to 37° for 3 hr. Cells were harvested and whole-cell protein extracts were made.

**Preparation of yeast cell extracts:** Yeast was grown in 50 ml of liquid SCD at 25° until they reached exponential growth ($10^7$ cells/ml). The cultures were then shifted to the nonpermissive temperature (37°) and grown for 4 hr. The cells were collected and yeast whole-cell extracts were prepared as described (Cai and Schmitt 2001).

**Western blot analysis:** SDS-PAGE was performed as previously described (Cai *et al.* 1999). A total of 40 μg of yeast protein extract was denatured in 2% (w/v) SDS, 5% (v/v) β-mercaptoethanol for 5 min at 95°, and resolved on a 15% (w/v) polyacrylamide gel. The anti-rabbit POD was detected with a Boehringer Mannheim (Indianapolis) chemiluminescence Western blotting kit and exposed to film for 10 min and then again overnight. Anti-Vma1 antibody, used as a loading control, was a kind gift of P. Kane (SUNY Upstate Medical University).

**Analysis of yeast RNA:** RNA was extracted as previously described (Schmitt *et al.* 1990). Approximately 10 μg of whole-cell RNA was separated on 1% (w/v) agarose gels or 6% (w/v) acrylamide/7 M urea gels (Sambrook *et al.* 1989). Gels were stained with ethidium bromide to visualize the 5.8S rRNA or Northern blot analysis was performed (Sambrook *et al.* 1989; Schmitt and Clayton 1993). Probes used for Northern analysis were *CLB2* (653-bp *Bgl*II-*Hin*dIII fragment of the *CLB2* gene; Fitch *et al.* 1992) and *ACT1* (1141-bp *Xho*I-*Kpn*I fragment of the *ACT1* gene; Shortle *et al.* 1982). Probes were radiolabeled for hybridization with [α-$^{32}$P]dCTP using the Prime-It Kit (Stratagene, La Jolla, CA). Radioactive blots were analyzed on a Molecular Dynamics (Sunnyvale, CA) PhosphoImager. Northern blots were probed a second time with actin to ensure equal loading.

**Construction of EFM and RNase MRP double mutants:** Strains carrying the *cdc5-1*, *cdc14-1*, and *cdc15-1* were the kind gift of D. Botstein, Stanford University. These strains were backcrossed to our strain background three times in the case of *cdc5* and four times for *cdc14* and *cdc15*. Haploid strains from the final cross carrying the relevant markers were used to shuffle in the different *NME1* and *SNM1* alleles as previously described (Cai *et al.* 1999; Shadel *et al.* 2000). Deletions for *clb1*, *clb2*, and *clb5* were obtained from Research Genetics (San Diego, CA). These double-mutant strains were generated in the same way as the *cdc*s.

**Growth tests of yeast mutants:** Mutant yeast strains were analyzed for temperature conditional growth on YPD media plates at 24°, 30°, 34°, and 37°. A total of 100 μl of sterile water was aliquoted to each well of a 96-well tissue culture plate. Two fresh colonies from each yeast strain were mixed into the first row wells. Tenfold serial dilutions of these cell mixtures were done in subsequent wells. A 48-pin Frogger (Dankar) was used to transfer diluted cell mixtures onto YPD media plates. The cells were grown at the temperatures specified for 3 days. All growth tests were performed at least three separate times in duplicates to ensure reproducibility.

## RESULTS

**Mutations in yeast RNase MRP components cause a cell cycle delay at the end of mitosis:** While studying RNase MRP from yeast, genes for several of the known

**TABLE 1**

**List of *S. cerevisiae* strains used in this study**

| Strain | Genotype | Source |
|---|---|---|
| THR200 | *MAT***a** *ade2 his3-Δ200 leu2-3, 112 trp1-Δ1 ura3-52 snm1-Δ1::HIS3 pTHR101 [URA3 CEN SNM1]* | Cai *et al.* (1999) |
| YGB30 | *MAT***a** *ade2 his3-Δ200 leu2-3, 112 trp1-Δ1 ura3-52 snm1Δ1::HIS3 pGAB119 [SNM1::GFP::6His LEU2 CEN]* | This study |
| YLL323 | *MAT***a**/α *ade2-101/ade2-101 his3-Δ200/his3-Δ200 ura3-52/ura3-52 TYR1/tyr1-1 lys2-1/LYS2 pop4Δ1::HIS3/POP4* | L. Lindahl (UMBC) |
| YGB26 | *MAT***a**/α *ade2-101/ade2-101 his3-Δ200/his3-Δ200 ura3-52/ura3-52 TYR1/tyr1-1 lys2-1/LYS2 pop4Δ1::HIS3/POP4 pSC93[POP4::HA URA3 CEN]* | This study |
| YGB26-14D | *MAT*α *ade2-101 his3-Δ200 leu2-3, 112 trp1-Δ1 ura3-52 pop4Δ1::HIS3 pSC93 [POP4::HA URA3 CEN]* | This study |
| MES101 | *MAT***a**/α *ADE2/ade2 LYS2/lys2-801 his3-Δ200/his3-Δ200 ura3-52/ura3-52 leu2-3, 112/leu2-3, 112 trp1-Δ1/trp1-Δ1* | Schmitt and Clayton (1992) |
| YGB22 | *MAT***a**/α *ADE2/ade2 LYS2/lys2-801 his3-Δ200/his3-Δ200 ura3-52/ura3-52 leu2-3, 112/leu2-3, 112 trp1-Δ1/trp1-Δ1 POP3/pop3Δ1::HIS3* | This study |
| YGB24 | *MAT***a**/α *ADE2/ade2 LYS2/lys2-801 his3-Δ200/his3-Δ200 ura3-52/ura3-52 leu2-3, 112/leu2-3, 112 trp1-Δ1/trp1-Δ1 POP3/pop3Δ1::HIS3 pTC143[POP3 URA3 CEN]* | This study |
| YGB24-38A | *MAT***a** *lys2-801 his3-Δ200 ura3-52 leu2-3, 112 trp1-Δ1 pop3Δ1::HIS3 pTC143 [POP3 URA3 CEN]* | This study |
| YGB28 | *MAT***a**/α *ADE2/ade2-101 LYS2/lys2-801 his3-Δ200/his3-Δ200 leu2-3, 112/leu2-3, 112 trp1-Δ1/trp1-Δ1 ura3-52/ura3-52 POP3/pop3Δ1::HIS3 POP4/pop4Δ1::HIS3* | This study |
| YGB29 | *MAT***a**/α *ADE2/ade2-101 LYS2/lys2-1 his3-Δ200/his3-Δ200 leu2-3, 112/leu2-3, 112 trp1-Δ1/trp1-Δ1 ura3-52/ura3-52 POP3/pop3Δ1::HIS3 POP4/pop4Δ1::HIS3 pGAB116[POP3::GFP POP4::3XHA URA3 CEN]* | This study |
| YGB29-4A | *MAT*α *lys2-801 trp1-Δ1 ura3-52 leu2-3, 112 his3-Δ200 pop3Δ1::HIS3 pop4Δ1::HIS3 pGAB116[POP3::GFP POP4::3XHA URA3 CEN]* | This study |
| MES250 | *MAT***a**/α *ADE2/ade2 LYS2/lys2-801 his3-Δ200/his3-Δ200 leu2-3, 112/leu2-3, 112 trp1-Δ1/trp1-Δ1 ura3-52/ura3-52 SNM1/snm1Δ1::HIS3 POP3/pop3Δ1::HIS3 POP4/pop4Δ1::HIS3 pGAB119[SNM1::GFP::6His LEU2 CEN] pGAB116 [POP3::GFP POP4::3XHA URA3 CEN]* | This study |
| YMC6 | *MAT***a** *ade2 trp1-Δ1 ura3-52 leu2-3, 112 his3-Δ200 pop3Δ1::HIS3 pop4::HIS3 snm1Δ1::HIS3 pGAB116[POP3::GFP POP4::3XHA URA3 CEN] pGAB119 [SNM1::GFP::6His LEU2 CEN]* | This study |
| MES300 | *MAT*α *lys2-801 his3-Δ200 leu2-3, 112 ura3-52 trp1-Δ1 nme1-Δ2::TRP1 pMES140 [NME1 LEU2 CEN)* | Shadel *et al.* (2000) |
| MES300-P6 | *MAT*α *lys2-801 his3-Δ200 leu2-3, 112 ura3-52 trp1-Δ1 nme1-Δ2::TRP1 pMES140-P6 (nme1-P6 LEU2 CEN)* | Shadel *et al.* (2000) |
| YTC150 | *MAT***a** *ade2 his3-Δ200 leu2-3, 112 trp1-Δ1 ura3-52 snm1-Δ1::HIS3 pTHR100 [LEU2 CEN SNM1]* | Cai *et al.* (1999) |
| YTC150-p18 | *MAT***a** *ade2-1 leu2-3, 112 his3-Δ200 trp1-Δ1 ura3-52 snm1-Δ1::HIS3 pTHR100-p18[snm1-p18 LEU2 CEN]* | Cai *et al.* (1999) |
| YTC150-172 | *MAT***a** *ade2-1 leu2-3, 112 his3-Δ200 trp1-Δ1 ura3-52 snm1-Δ1::HIS3 pTC172 [snm1-172 LEU2 CEN]* | Cai *et al.* (1999) |
| MES111 | *MAT*α *his3-Δ200 leu2-3, 112 ura3-52 trp1-Δ1 ade2 nme1-Δ2::TRP1 pMES127 [URA3CEN NME1]* | Schmitt and Clayton (1994) |
| MES111-140 | *MAT*α *his3-Δ200 leu2-3, 112 ura3-52 trp1-Δ1 ade2 nme1-Δ2::TRP1 pMES140 [CEN LEU2 NME1]* | Schmitt and Clayton (1994) |
| MES111-P6 | *MAT*α *his3-Δ200 leu2-3, 112 ura3-52 trp1-Δ1 ade2 nme1-Δ2::TRP1 pMES140-P6 [CEN LEU2 nme1-P6]* | Schmitt and Clayton (1994) |
| MES111-140 + pTC185 | *MAT*α *his3-Δ200 leu2-3, 112 ura3-52 trp1-Δ1 ade2 nme1-Δ2::TRP1 pMES140 [CEN LEU2 NME1] pTC185[ADE2 URA3 CEN]* | This study |
| MES111-P6 + pTC185 | *MAT*α *his3-Δ200 leu2-3, 112 ura3-52 trp1-Δ1 ade2 nme1-Δ2::TRP1 pMES140-P6[CEN LEU2 nme1-P6] pTC185[ADE2 URA3 CEN]* | This study |
| E2 | *MAT***a** *ade2-1 his3-1115 ura3-1 leu2-3, 112 trp1-1 can1-100 CLB2::3XHA* | R. Hallberg Syracuse Univ. |
| MES116 | *MAT*α *lys2-801 his3-Δ200 leu2-3, 112 ura3-52 trp1-Δ1 nme1-Δ2::TRP1 pMES127 [URA3CEN NME1]* | Schmitt and Clayton (1992) |

(*continued*)

**TABLE 1**

**(Continued)**

| Strain | Genotype | Source |
|---|---|---|
| YTC220 | *MAT***a**/α *ADE2/ade2-1 LYS2/lys2-801 his3-Δ200/his3-1115 leu2-3, 112/leu2-3, 112 ura3-52/ura3-1 trp1-1/trp1-Δ1 NME1/nme1-Δ2::TRP1 CLB2/CLB2::3XHA pMES127[URA3CEN NME1]* | This study |
| YTC220-1A | *MAT*α *lys2-801 his3 leu2-3, 112 ura3 trp1 nme1-Δ2::TRP1 CLB2::3XHA pMES127[URA3CEN NME1]* | This study |
| YTC221 | *MAT*α *lys2-801 his3 leu2-3, 112 ura3 trp1 nme1-Δ2::TRP1 CLB2::3XHA pMES140 [CEN LEU2 NME1]* | This study |
| YTC222 | *MAT*α *lys2-801 his3 leu2-3, 112 ura3 trp1 nme1-Δ2::TRP1 CLB2::3XHA pMES140-P6[CEN LEU2 nme1-P6]* | This study |
| MES117 | *MAT***a** *lys2-801 his3-Δ200 leu2-3, 112 ura3-52 trp1-Δ1 nme1-Δ2::TRP1 pMES127[URA3CEN NME1]* | This study |
| YTC240 | *MAT***a** *lys2-801 his3-Δ200 leu2-3, 112 ura3-52 trp1-Δ1 CDC14::GFP nme1-Δ2::TRP1 pMES127[URA3CEN NME1]* | This study |
| YTC241 | *MAT***a** *lys2-801 his3-Δ200 leu2-3, 112 ura3-52 trp1-Δ1 CDC14::GFP nme1-Δ2::TRP1 pMES140[CEN LEU2 NME1] pTS403[CEN URA3 TUB3::GFP]* | This study |
| YTC242 | *MAT***a** *lys2-801 his3-Δ200 leu2-3, 112 ura3-52 trp1-Δ1 CDC14::GFP nme1-Δ2::TRP1 pMES140-P6[CEN LEU2 nme1-P6] pTS403[CEN URA3 TUB3::GFP]* | This study |
| YJA101 | *MAT*α *ade2-1 his3-Δ200 leu2-3, 112 met15 trp1-Δ1 ura3-52 nme1-Δ2::TRP1 clb2Δ::KanMX4 pMES127 [URA3 CEN NME1]* | This study |
| YJA102 | *MAT***a** *lys2-1 his3-Δ200 leu2-3, 112 met15 trp1-Δ1 ura3-52 snm1-Δ1::HIS3 clb2Δ::KanMX4 pMES202 [URA3 2μ SNM1]* | This study |
| YJA103 | *MAT*α *ade2-1 his3-Δ200 leu2-3, 112 met15 trp1-Δ1 ura3-52 nme1-Δ2::TRP1 clb2Δ::KanMX4 pMES140 [LEU2 CEN NME1]* | This study |
| YJA104 | *MAT*α *ade2-1 his3-Δ200 leu2-3, 112 met15 trp1-Δ1 ura3-52 nme1-Δ2::TRP1 clb2Δ::KanMX4 pMES140-Δ2 [LEU2 CEN nme1-Δ2]* | This study |
| YJA105 | *MAT*α *ade2-1 his3-Δ200 leu2-3, 112 met15 trp1-Δ1 ura3-52 nme1-Δ2::TRP1 clb2Δ::KanMX4 pMES140-P6 [LEU2 CEN nme1-p6]* | This study |
| YJA106 | *MAT***a** *lys2-1 his3-Δ200 leu2-3, 112 met15 trp1-Δ1 ura3-52 snm1-Δ1::HIS3 clb2Δ::KanMX4 pTC120 [LEU2 CEN SNM1]* | This study |
| YJA107 | *MAT***a** *lys2-1 his3-Δ200 leu2-3, 112 met15 trp1-Δ1 ura3-52 snm1-Δ1::HIS3 clb2Δ::KanMX4 pTC172[snm1-172 LEU2 CEN]* | This study |
| YJA108 | *MAT***a** *lys2-1 his3-Δ200 leu2-3, 112 met15 trp1-Δ1 ura3-52 snm1-Δ1::HIS3 clb2Δ::KanMX4 pTHR100-p18[snm1-p18 LEU2 CEN]* | This study |
| YJA111 | *MAT***a** *his3-Δ200 leu2-3, 112 met15 trp1-Δ1 ura3-52 nme1-Δ2::TRP1 clb1Δ::KanMX4 pMES127 [URA3 CEN NME1]* | This study |
| YJA112 | *MAT***a** *lys2-1 his3-Δ200 leu2-3, 112 met15 trp1-Δ1 ura3-52 snm1-Δ1::HIS3 clb1Δ::KanMX4 pMES202 [URA3 2( SNM1]* | This study |
| YJA113 | *MAT***a** *his3-Δ200 leu2-3, 112 met15 trp1-Δ1 ura3-52 nme1-Δ2::TRP1 clb1Δ::KanMX4 pMES140 [LEU2 CEN NME1]* | This study |
| YJA114 | *MAT***a** *his3-Δ200 leu2-3, 112 met15 trp1-Δ1 ura3-52 nme1-Δ2::TRP1 clb1Δ::KanMX4 pMES140-Δ2 [LEU2 CEN nme1-Δ2]* | This study |
| YJA115 | *MAT***a** *his3-Δ200 leu2-3, 112 met15 trp1-Δ1 ura3-52 nme1-Δ2::TRP1 clb1Δ::KanMX4 pMES140-P6 [LEU2 CEN nme1-p6]* | This study |
| YJA116 | *MAT***a** *lys2-1 his3-Δ200 leu2-3, 112 met15 trp1-Δ1 ura3-52 snm1-Δ1::HIS3 clb1Δ::KanMX4 pTC120 [LEU2 CEN SNM1]* | This study |
| YJA117 | *MAT***a** *lys2-1 his3-Δ200 leu2-3, 112 met15 trp1-Δ1 ura3-52 snm1-Δ1::HIS3 clb1Δ::KanMX4 pTC172[snm1-172 LEU2 CEN]* | This study |
| YJA118 | *MAT***a** *lys2-1 his3-Δ200 leu2-3, 112 met15 trp1-Δ1 ura3-52 snm1-Δ1::HIS3 clb1Δ::KanMX4 pTHR100-p18[snm1-p18 LEU2 CEN]* | This study |
| YJA121 | *MAT*α *ade2-1 his3-Δ200 leu2-3, 112 met15 trp1-Δ1 ura3-52 nme1-Δ2::TRP1 clb5Δ::KanMX4 pMES127 [URA3 CEN NME1]* | This study |
| YJA122 | *MAT*α *lys2-1 his3-Δ200 leu2-3, 112 met15 trp1-Δ1 ura3-52 snm1-Δ1::HIS3 clb5Δ::KanMX4 pMES202 [URA3 2μ SNM1]* | This study |
| YJA123 | *MAT*α *ade2-1 his3-Δ200 leu2-3, 112 met15 trp1-Δ1 ura3-52 nme1-Δ2::TRP1 clb5Δ::KanMX4 pMES140 [LEU2 CEN NME1]* | This study |
| YJA124 | *MAT*α *ade2-1 his3-Δ200 leu2-3, 112 met15 trp1-Δ1 ura3-52 nme1-Δ2::TRP1 clb5Δ::KanMX4 pMES140-Δ2 [LEU2 CEN nme1-Δ2]* | This study |

(*continued*)

**TABLE 1**

**(Continued)**

| Strain | Genotype | Source |
|---|---|---|
| YJA125 | *MATα ade2-1 his3-Δ200 leu2-3, 112 met15 trp1-Δ1 ura3-52 nme1-Δ2::TRP1 clb5Δ::KanMX4 pMES140-P6 [LEU2 CEN nme1-p6]* | This study |
| YJA126 | *MATα lys2-1 his3-Δ200 leu2-3, 112 met15 trp1-Δ1 ura3-52 snm1-Δ1::HIS3 clb5Δ::KanMX4 pTC120 [LEU2 CEN SNM1]* | This study |
| YJA127 | *MATα lys2-1 his3-Δ200 leu2-3, 112 met15 trp1-Δ1 ura3-52 snm1-Δ1::HIS3 clb5Δ::KanMX4 pTC172[snm1-172 LEU2 CEN]* | This study |
| YJA128 | *MATα lys2-1 his3-Δ200 leu2-3, 112 met15 trp1-Δ1 ura3-52 snm1-Δ1::HIS3 clb5Δ::KanMX4 pTHR100-p18[snm1-p18 LEU2 CEN]* | This study |
| TLG129 | *MATα ade2-1 his3-Δ200 leu2-3, 112 lys2-1 trp1-Δ1 ura3-52 nme1-Δ2::TRP1 cdc14-1 pMES127 [URA3 CEN NME1]* | This study |
| TLG133 | *MATα ade2-1 his3-Δ200 leu2-3, 112 trp1-Δ1 ura3-52 nme1-Δ2::TRP1 cdc15-1 pMES127[URA3 CEN NME1]* | This study |
| TLG179 | *MATα ade2-1 his3-Δ200 leu2-3, 112 lys2-1 trp1-Δ1 ura3-52 nme1-Δ2::TRP1 cdc5-1 pMES127[URA3 CEN NME1]* | This study |
| TLG180 | *MATα ade2-1 his3-Δ200 leu2-3, 112 lys2-1 trp1-Δ1 ura3-52 nme1-Δ2::TRP1 cdc14-1 pMES140[CEN LEU2 NME1]* | This study |
| TLG181 | *MATα ade2-1 his3-Δ200 leu2-3, 112 lys2-1 trp1-Δ1 ura3-52 nme1-Δ2::TRP1 cdc14-1 pMES140-Δ2[CEN LEU2 nme1-Δ2]* | This study |
| TLG182 | *MATα ade2-1 his3-Δ200 leu2-3, 112 lys2-1 trp1-Δ1 ura3-52 nme1-Δ2::TRP1 cdc14-1 pMES140-P6[CEN LEU2 nme1-P6]* | This study |
| TLG183 | *MATα ade2-1 his3-Δ200 leu2-3, 112 trp1-Δ1 ura3-52 nme1-Δ2::TRP1 cdc15-1 pMES140[CEN LEU2 NME1]* | This study |
| TLG184 | *MATα ade2-1 his3-Δ200 leu2-3, 112 trp1-Δ1 ura3-52 nme1-Δ2::TRP1 cdc15-1 pMES140-Δ2[CEN LEU2 nme1-Δ2]* | This study |
| TLG185 | *MATα ade2-1 his3-Δ200 leu2-3, 112 trp1-Δ1 ura3-52 nme1-Δ2::TRP1 cdc15-1 pMES140-P6[CEN LEU2 nme1-P6]* | This study |
| TLG186 | *MATα ade2-1 his3-Δ200 leu2-3, 112 lys2-1 trp1-Δ1 ura3-52 nme1-Δ2::TRP1 cdc5-1 pMES140[CEN LEU2 NME1]* | This study |
| TLG187 | *MATα ade2-1 his3-Δ200 leu2-3, 112 lys2-1 trp1-Δ1 ura3-52 nme1-Δ2::TRP1 cdc5-1 pMES140-Δ2[CEN LEU2 nme1-Δ2]* | This study |
| TLG188 | *MATα ade2-1 his3-Δ200 leu2-3, 112 lys2-1 trp1-Δ1 ura3-52 nme1-Δ2::TRP1 cdc5-1 pMES140-P6[CEN LEU2 nme1-P6]* | This study |
| TLG141 | *MATα lys2-1 his3-Δ200 leu2-3, 112 trp1-Δ1 ura3-52 snm1-Δ1::HIS3 cdc14-1 pMES202 [URA3 2μ SNM1]* | This study |
| TLG137 | *MATα ade2-1 lys2-1 his3-Δ200 leu2-3, 112 trp1-Δ1 ura3-52 snm1-Δ1::HIS3 cdc15-1 pMES202 [URA3 2μ SNM1]* | This study |
| TLG178 | *MATα ade2-1 lys2-1 his3-Δ200 leu2-3, 112 trp1-Δ1 ura3-52 snm1-Δ1::HIS3 cdc5-1 pMES202 [URA3 2μ SNM1]* | This study |
| TLG189 | *MATα lys2-1 his3-Δ200 leu2-3, 112 trp1-Δ1 ura3-52 snm1-Δ1::HIS3 cdc14-1 pTC120 [LEU2 CEN SNM1]* | This study |
| TLG190 | *MATα lys2-1 his3-Δ200 leu2-3, 112 trp1-Δ1 ura3-52 snm1-Δ1::HIS3 cdc14-1 pTC172[snm1-172 LEU2 CEN]* | This study |
| TLG191 | *MATα lys2-1 his3-Δ200 leu2-3, 112 trp1-Δ1 ura3-52 snm1-Δ1::HIS3 cdc14-1 pTHR100-p18[snm1-p18 LEU2 CEN]* | This study |
| TLG192 | *MATα ade2-1 lys2-1 his3-Δ200 leu2-3, 112 trp1-Δ1 ura3-52 snm1-Δ1::HIS3 cdc15-1 pTC120[LEU2 CEN SNM1]* | This study |
| TLG193 | *MATα ade2-1 lys2-1 his3-Δ200 leu2-3, 112 trp1-Δ1 ura3-52 snm1-Δ1::HIS3 cdc15-1 pTC172[snm1-172 LEU2 CEN]* | This study |
| TLG194 | *MATα ade2-1 lys2-1 his3-Δ200 leu2-3, 112 trp1-Δ1 ura3-52 snm1-Δ1::HIS3 cdc15-1 pTHR100-p18[snm1-p18 LEU2 CEN]* | This study |
| TLG195 | *MATα ade2-1 lys2-1 his3-Δ200 leu2-3, 112 trp1-Δ1 ura3-52 snm1-Δ1::HIS3 cdc5-1 pTC120[LEU2 CEN SNM1]* | This study |
| TLG196 | *MATα ade2-1 lys2-1 his3-Δ200 leu2-3, 112 trp1-Δ1 ura3-52 snm1-Δ1::HIS3 cdc5-1 pTC172[snm1-172 LEU2 CEN]* | This study |

protein subunits of the complex were fused to the gene for GFP, GFP-6 histidine (*GFP::6HIS*), or hemaglutinin (HA) and used to replace the wild-type copies of the respective genes in yeast cells (Figure 1A). The fluorescent tags allow for cellular localization of the RNase MRP components. Each of the tagged components was

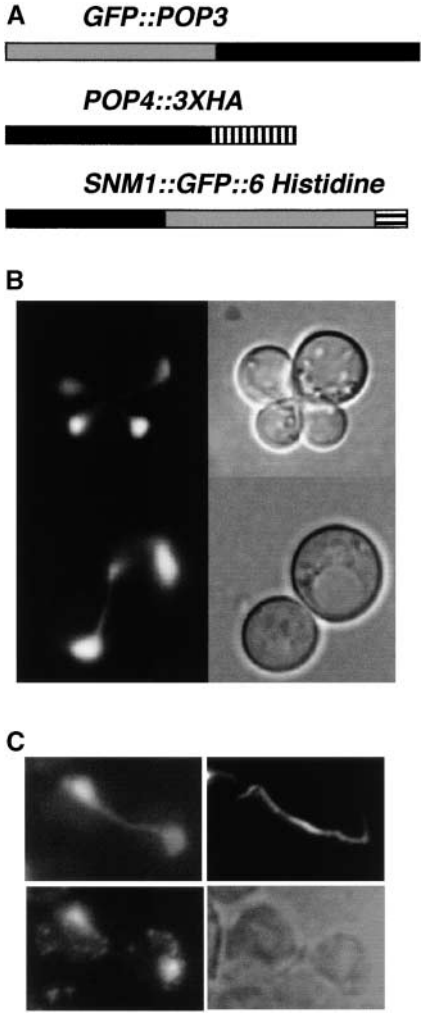


FIGURE 1.—(A) Schematic of protein fusions present in the YMC6 strain. The genes for three of the known protein subunits of RNase MRP were fused to GFP, GFP:6HIS, or three copies of the HA epitope (CHU *et al.* 1997; gift of Lasse Lindahl, University of Maryland, Baltimore County) and used to replace the wild-type copies of the respective genes in yeast cells. The yeast strain YMC6 contains replacements of all three subunits shown simultaneously, *SNM1::GFP::6HIS*, *POP3::GFP*, and *POP4::3×HA*. (B) Examples of the cell cycle delay observed in the YMC6 strain. The GFP fluorescence localized to the nucleus. The YMC6 strain was grown to $10^6$ cells/ml at 30° in YPD and cells were examined under a fluorescence microscope with a GFP filter set. Observed fluorescence is on the left and differential interference contrast is on the right. Approximately 40% of the cells display the morphology shown. (C) Simultaneous localization of GFP staining, mitotic spindle, and DNA in telophase-arrested YMC6 (see MATERIALS AND METHODS). Clockwise from the top left is GFP fluorescence, Cy3-staining tubulin, visible light, and DNA stained with DAPI.

able to complement a strain deleted for the original gene and grew as well as the original wild-type strain. However, a strain designated YMC6, which expressed all three tagged subunits simultaneously, showed a significantly increased generation time at 30° and marked temperature sensitivity at 37°. The GFP-tagged subunits corresponding to the *GFP::POP3* localized to the nucleus, providing bright nuclear fluorescence (Figure 1B). Microscopic observation of YMC6 at 30° (semipermissive) and, in particular, at 37° (nonpermissive) revealed an accumulation of cells at a late stage of the cell cycle. This stage of the cell cycle was exemplified by an hourglass-shaped nucleus (Figure 1B). Cells grown at 30° and shifted to 37° for 4 hr displayed an increased number of large-budded cells with dumbbell-shaped nuclei and what appeared to be an extended, contiguous spindle. This cell cycle arrest phenotype is identical to that displayed by the class of M-to-$G_1$ transition genes involved in the exit from mitosis (ZACHARIAE and NASMYTH 1999). Mutants in these genes have been shown to arrest in telophase with well-divided DNA, an hourglass-shaped nucleus, and an extended mitotic spindle (SURANA *et al.* 1993). As can be seen in Figure 1C, this is also the case for the telophase-arrested cells in the YMC6 strain.

Since two of the tagged-protein components in the YMC6 strain are shared with RNase P, we examined whether the phenotype was the result of an RNase MRP defect alone. A strain carrying the temperature-conditional MRP RNA mutation, *nme1-P6*, which has a point mutation (G-to-A transition at position 122 of MRP RNA) in the *NME1* gene (SCHMITT and CLAYTON 1993; SHADEL *et al.* 2000), was examined for a cell cycle defect. We used 4′,6-diamidino-2-phenylindole (DAPI) staining to visualize DNA and an anti-tubulin antibody to visualize the mitotic spindle allowing for easy cell cycle staging. To a greater extent than the YMC6 strain, cells built up with large budded cells, a long mitotic spindle, and divided DNA (Figure 2). In addition, a strain carrying the temperature-sensitive mutation in the *SNM1* gene, *snm1-p18*, displayed a similar phenotype (Figure 2 and CAI *et al.* 1999). Snm1 is a protein component RNase MRP and not a component of RNase P (SCHMITT and CLAYTON 1994; CHAMBERLAIN *et al.* 1998). Random fields of 200 cells were scored for their stage in the cell cycle. In the wild type we found that ~9.5% of cells were in telophase at any one time, with long spindles and divided DNA. The strain with the *nme1-P6* mutation and the YMC6 strain both have a much higher percentage of cells in telophase even at the semipermissive temperature of 30°, 71 and 39%, respectively. These results indicate a cell cycle delay as opposed to a 100% arrest.

**Plasmid missegregation in RNase MRP RNA mutants:** It has been demonstrated that mutations in the Snm1 protein will cause a plasmid segregation problem (CAI *et al.* 1999). This missegregation may be caused by a prolonged cell cycle arrest at telophase caused by the loss of RNase MRP function. In addition, other EFM mutants also have plasmid segregation problems (HARDY and PAUTZ 1996; SHOU and DESHAIES 2002). Because of this we tested plasmid segregation in a strain with the *nme1-P6* mutation. The reporter plasmid pTC185, which contains a wild-type *ADE2* gene in the *CEN/URA3*

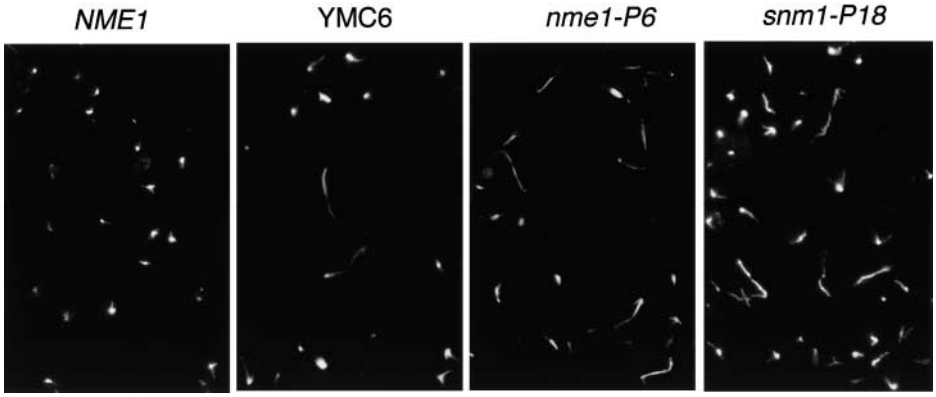


FIGURE 2.—Immunolocalization of mitotic spindles in the strain YMC6 and RNase MRP RNA and protein mutants. Yeast strains were grown to $2 \times 10^6$ cells/ml at 30° in YPD. The *snm1-P18* strain was shifted to 37° for an additional 3 hr before harvesting (CAI *et al.* 1999). Cells were fixed and the mitotic spindle and DNA were localized (see MATERIALS AND METHODS). Cy3-staining tubulin is shown. *NME1*(wild type), MES111-140; *nme1-P6*, MES111-P6; *snm1-p18*, YTC150-p18.

vector pRS316 (CAI *et al.* 1999), was transformed into both a wild-type and *nme1-P6* strain. Because of a *ade2-1* mutation on the chromosome, these strains normally form red colonies on YPD plates. However, after having been transformed with the plasmid pTC185 containing the *ADE2* gene, they form white colonies. Loss of the plasmid during colony growth produces red sectors in white colonies. If there is a segregation problem, an increase in the number of red sectors is expected.

The results are shown in Figure 3. Most wild-type cells are white, although a small number of red colonies are observed due to plasmid loss during the nonselective growth. A few sectoring colonies are found, most of which have fewer than two small sectors. In the *nme1-P6* strain a large increase in plasmid missegregation is observed, as indicated by the increase in the number of colonies with multiple sectors. The sectoring results demonstrate that defects in the MRP RNA can cause plasmid missegregation. On the basis of our cell cycle delay findings, it is predicted that the missegregation is the result of a prolonged period of telophase in RNase MRP mutants even at the permissive temperature.

***CDC5* was identified as a suppressor of the *snm1-172* mutation:** *snm1-172* is a temperature-sensitive, site-directed mutation (Cys64 to Ala) of the unique RNase MRP protein component Snm1p. A strain carrying the *snm1-172* mutation is temperature sensitive and shows a 5.8S rRNA processing defect characteristic of RNase MRP mutants (CAI *et al.* 1999). Because this mutant both contained a single missense mutation and displayed strong temperature sensitivity, we used it to perform a high-copy suppressor search for new proteins involved in MRP function. A yeast 2μ library was transformed into the *snm1-172* strain, and library transformants were selected on uracil minus medium, replicated, and grown at 37° for 3 days. A single suppressor clone was identified four times independently. The suppressor was retested, sequenced, and found to contain a 9.3-kb genomic DNA fragment of chromosome XIII (Figure 4A). The insert was subcloned and subjected to deletion analysis. A shorter fragment containing the *CDC5* gene and *CEN13* (Sph1Δ) gave the same strong suppression as the original clone; however, the *CDC5* gene alone gave only weak suppression of the *snm1-172* mutation. It is known that high-level overexpression of *CDC5* will result in growth arrest with a nonuniform terminal phenotype in yeast cells (CHARLES *et al.* 1998), and the presence of the *CEN13* may reduce the copy number of the 2μ plasmid to a lower level and provide better suppression. To confirm that *CDC5* is the suppressor gene, a fragment in the *CDC5* open reading frame was removed in the Sph1Δ clone and this construct was tested. It did not suppress the s*nm1-172* mutation nor did *CEN13* alone (Figure 4B). Cdc5, a polo-like kinase, is a high-copy suppressor of many EFM mutants, including *cdc15*, *tem1*, and *dbf2* (KITADA *et al.* 1993; JASPERSEN *et al.* 1998). Overexpression of *CDC5* has been shown to promote the destruction of Clb2, the B-type cyclin whose proteolysis allows progression from anaphase to $G_1$ (CHARLES *et al.* 1998).

A strain carrying the *snm1-172* mutation has previously been shown to have a distinct rRNA processing defect, and the small-to-large 5.8S rRNA ratio was changed from the normal 10:1 ratio (CAI *et al.* 1999). We examined rRNA processing when the *snm1-172* mutation is being suppressed by a high-copy *CDC5* gene. Identical to the strain without the suppressor, the 5.8S rRNA ratio was

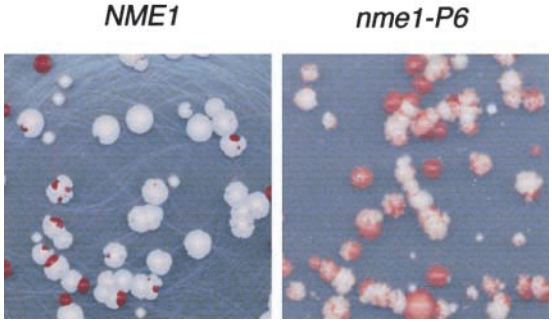


FIGURE 3.—Plasmid segregation in a RNase MRP RNA mutant. The *nme1-P6* mutant yeast strain was transformed with a plasmid carrying a wild-type *ADE2* gene so that plasmid stability could be monitored by a simple color assay (see MATERIALS AND METHODS; CAI *et al.* 1999). Pictures were taken after 3 days growth at 30° (a semipermissive temperature for the *nme1-P6* mutant). *NME1* (wild type), MES111-140 + pTC185; *nme1-P6*, MES111-P6 + pTC185.

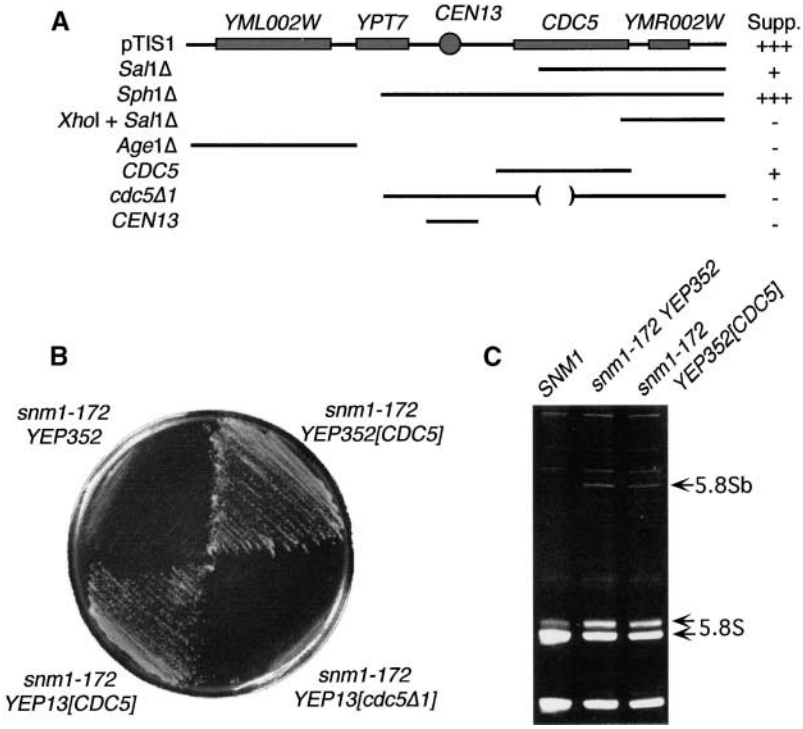


FIGURE 4.—CDC5 is a high-copy suppressor of the *snm1-172* mutation. (A) Map of the genomic DNA insert found as a high-copy suppressor of the *snm1-172* mutation. The *snm1-172* mutation is a strong temperature-sensitive point mutation in the *SNM1* gene (CAI *et al.* 1999). A gene map of the original suppressing clone is shown. The lines below the map represent fragments of this region that were tested for suppression of the *snm1-172* mutation when in the yeast 2μ/*URA3* vector YEP352. The ability of these clones to suppress is indicated by a (−), no suppression; (+), partial suppression; or (+++), suppression at 37°. (B) Suppressor clone with a deletion in *CDC5* coding region cannot suppress the *snm1-172* mutation. Yeast cells were spread onto SCD plates at 37° and grown for 24 hr before photographing. Yeast strain YTC150-172, which carries the *snm1-172* mutation, was tested with an empty YEP352 vector (YEP352), the *CDC5* gene (*Sph*1Δ, in Figure 4A) on YEP352 or YEP13, or a deletion in the *CDC5* coding region (YEP13 [*cdc5*Δ1]). (C) The *CDC5* suppressor restores cell growth but has no effect on the defect in ribosomal RNA processing in the *snm1-172* mutant. Yeast strains were grown to $2 \times 10^7$ cells/ml at 24° in YPD and then shifted to 37° for 4 hr. Total RNA was isolated, and equal amounts were separated on a 6% acrylamide/7 M urea gel and stained with ethidium bromide (SCHMITT *et al.* 1990). The locations of the relevant 5.8S, small and large, and 5.8Sb rRNAs are indicated (SCHMITT and CLAYTON 1993). Strains are the same as in B; *SNM1*, YTC150.

altered, and an aberrant precursor (5.8Sb; SCHMITT and CLAYTON 1993) was observed (Figure 4C). The amounts of the individual bands were quantitated on a BioRad Fluor-S MultiImager using Bio-Rad's Quantity One quantitation software, with the 5S rRNA as a loading standard, and found to have no significant difference between the *snm1-172* mutant and the *snm1-172* carrying the high-copy *CDC5*. These results indicate that *CDC5* suppresses the mutation through an alternate pathway from the known rRNA processing activity. It also suggests that the temperature-sensitive growth arrest caused by the *snm1-172* mutation is not the result of defective rRNA processing.

**Increase of Clb2 protein level in an RNase MRP RNA mutant:** The EFM mutants or M-to-$G_1$ mutant group (HARTWELL *et al.* 1974) all show higher mitotic cyclin levels and a resultant increased cyclin kinase activity (JASPERSEN *et al.* 1998). Clb2, the major mitotic cyclin in yeast at this stage in the cell cycle, has increased protein levels (two- to fourfold) in these mutants. To examine the Clb2 protein level, we replaced the *CLB2* gene in our strain background with a 3× HA-tagged *CLB2* gene (gift of R. Hallberg, Syracuse University; SHU *et al.* 1997). This allowed us to examine Clb2 protein using an anti-HA antibody (see Figure 5). In asynchronous cells the Clb2 protein level increased about two- to fourfold (as quantitated by densitometry) in the *nme1-P6* mutant as compared to the wild-type control. However, in hydroxyurea and nocodazole (drugs that arrest cells in S phase and M phase, respectively) Clb2 protein levels show no significant difference between wild-type and mutant cells, similar to the other EFM mutants. These changes were reproducible in six separate experiments and are a characteristic of most EFM mutants (JASPERSEN *et al.* 1998). This increase in B-cyclin protein confirms that cells are delaying at the end of mitosis. The cell cycle delay found in EFM mutants is due to accumu-

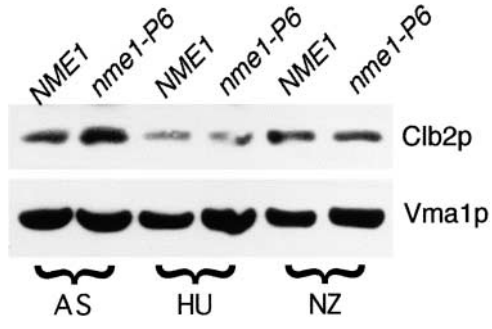


FIGURE 5.—Western analysis of Clb2 protein in a RNase MRP RNA mutant. Wild-type (*NME1*, YTC221) and *nme1-P6* (YTC222) mutant strains were grown to $10^6$ cells/ml at 25° in SCD. Cultures were then either directly shifted to 37° for 3 hr (AS) or first arrested in hydroxyurea (HU) or nocodazole (NZ) for 3 hr followed by the shift to 37° (see MATERIALS AND METHODS). Cells were harvested and whole-cell protein extracts were made, and Western analysis was performed. The HA-tagged Clb2 was detected with an anti-HA monoclonal antibody, followed by a mouse anti-Vma1 antibody as a loading control (gift of Dr. P. Kane, SUNY Upstate Medical University). The Clb2p band is indicated.

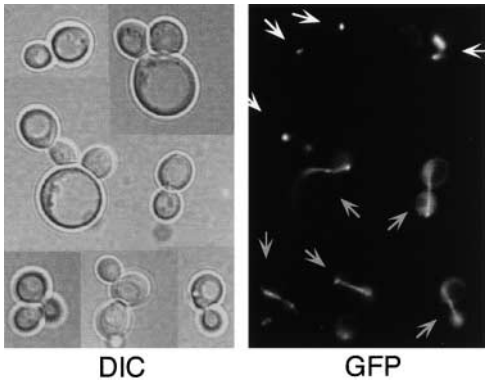


FIGURE 6.—Immunolocalization of Cdc14p in a RNase MRP mutant. A yeast strain carrying the *nme1-P6* mutation (YTC242) was grown to $2 \times 10^6$ cells/ml at 24° in YPD and shifted to 37° for 4 hr. The mitotic spindle was visualized using a *TUB3-GFP* gene that allowed easy cell cycle staging. Cdc14 was localized using a *CDC14-GFP* gene. Nucleolar staining of Cdc14p in nontelophase cells is indicated by the white arrows. Cells in telophase (which predominate in the mutant) are identified by the long mitotic spindle and diffuse cdc14p throughout the cell (gray arrows). (Left) Phase contrast; (right) GFP fluorescence.

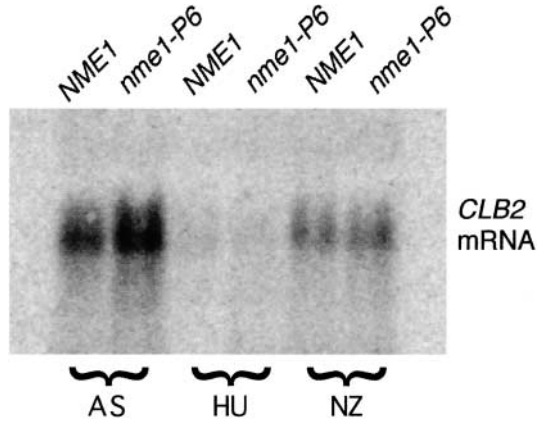


FIGURE 7.—Northern analysis of *CLB2* mRNA in *nme1-P6* cells. Wild-type (MES111-140) and *nme1-P6* (MES111-P6) mutant strains were prepared as in Figure 5 (see MATERIALS AND METHODS). Total RNA was isolated and equal amounts of total RNA were subjected to Northern analysis. Location of the *CLB2* transcript is indicated. AS, asynchronous cells; HU, hydroxyurea-synchronized cells; NZ, nocodazole-synchronized cells.

lation of B-cyclin protein in telophase. It is removal of this B-cyclin that is required to allow cells to exit from mitosis.

**Cdc14 localization was unaffected in a RNase MRP RNA mutant:** Cdc14 is a protein phosphatase that activates the degradation of Clb2 protein by dephosphorylation of the Hct1/Cdh1 protein, allowing it to bind and activate Clb2-directed APC/C degradation (VISINTIN *et al.* 1998). Cdc14 is sequestered in the nucleolus for most of the cell cycle and released from nucleolus during anaphase (SHOU *et al.* 1999; VISINTIN *et al.* 1999). RNase MRP is also located in the nucleolus where it processes ribosomal RNA precursors (REIMER *et al.* 1988; SCHMITT and CLAYTON 1993). We examined the possibility that a defect in RNase MRP could affect release of Cdc14 from the nucleolus and in turn affect exit from mitosis. We followed the Cdc14 protein by fusing the coding region for the GFP to the 3′ end of the endogenous *CDC14* gene (LONGTINE *et al.* 1998). This fusion gene was used to replace the wild-type gene. Cells were grown at permissive temperature to mid-log phase and then shifted to nonpermissive temperature for the *nme1-P6* mutation for 4 hr. Cdc14 localization was examined by fluorescence microscopy. To easily stage cells that were in telophase, we visualized the mitotic spindles by transforming cells with a tubulin-GFP plasmid (gift of D. Amberg, SUNY Upstate Medical University). In both wild-type and mutant cells, Cdc14 was localized in the nucleolus during most of the cell cycle (Figure 6, white arrows) and was released from the nucleolus late in telophase (Figure 6, gray arrows). This indicated that the cell cycle delay of a mutation in RNase MRP is not caused by a failure to mobilize the Cdc14 phosphatase.

**Increase of CLB2 mRNA levels in an RNase MRP RNA mutant:** RNase MRP is a well-characterized endoribonuclease (CHANG and CLAYTON 1987). We predict that the function of RNase MRP in the cell cycle involves the processing of some cellular RNA. We examined whether the *CLB2* mRNA level might be altered in a strain carrying the *nme1-P6* mutation (MES111-P6). Northern analysis was performed on asynchronous and drug-arrested populations of cells. As shown in Figure 7, in asynchronous cultures the *CLB2* mRNA level is three- to fourfold higher (as quantitated on a phosphoimager) in mutant cells than in wild-type cells. *CLB2* mRNA levels are not significantly different in either hydroxyurea- or nocodazole-arrested cells. This result is very similar to the changes that were seen at the protein level, suggesting that the increased mRNA level is the direct cause of the increased Clb2 protein levels leading to the block in cell cycle progression. It should be noted that this result is in contrast to a *cdc15* mutant (exit from mitosis mutant) that has been shown to have very low or undetectable levels of the *CLB2* mRNA when arrested at the nonpermissive temperature (FITCH *et al.* 1992; SPELLMAN *et al.* 1998).

**Genetic interactions of RNase MRP mutants with EFM mutants and mitotic cyclins:** Because of the phenotypic resemblance of RNase MRP mutants to EFM mutants and the high-copy suppression with *CDC5* we investigated various genetic interactions between mutations in EFM genes and mutations in RNase MRP genes. Temperature-sensitive mutations in *cdc5*, *-14*, and *-15* and deletions of *clb1*, *-2*, and *-5* were combined individually with RNase MRP mutants. These analyses of RNase MRP and EFM double mutants produced a number of genetic interactions. Double mutants were generated with four separate MRP mutants, *nme1-P6*, *nme1-Δ2*, *snm1-P18*, and *snm1-172* (CAI *et al.* 1999; SHADEL *et al.* 2000). All four

of these mutants are temperature sensitive for growth at 37°. The *nme1-P6* and *snm1-P18* mutants are strong mutants in terms of slow growth and defects in rRNA processing. The *nme1-Δ2* and the *snm1-172* are milder mutants in that they have normal growth rates at permissive temperatures and moderate rRNA processing defects. *CLB1* and *CLB2* are functionally redundant cyclins; however, *CLB2* is the major cyclin of this pair (Clb2p is at twice the level of Clb1p; Cross *et al.* 2002). *CLB5* has partially overlapping functions with *CLB1* and *CLB2* but is expressed in an earlier pattern in the cell cycle. Alone none of the *clb*Δs display a growth phenotype except the *clb2*Δ that is mildly temperature sensitive.

The *clb1*Δ was found to partially suppress all of the mutants tested except the *snm1-P18* that had a worsening of its growth defect. The *clb2*Δ was found to cause all the mutants to grow much more slowly, with the *nme1-P6/clb2*Δ and the *snm1-P18/ clb2*Δ strains growing extremely slowly and at only 25° (see Figure 8). The two weaker mutations demonstrated an increase in temperature sensitivity when combined with the *clb2*Δ. The clb5Δ was able to dramatically suppress the two stronger mutants.

Crosses between RNase MRP mutants and the EFM mutants *cdc14* and *cdc15* yielded synthetic interactions only with the *snm1-p18* mutant. A weak suppression of *cdc15-1* temperature sensitivity by mutations in *snm1* (Figure 9, right panel) was also seen. On the basis of our previously identified suppression of an RNase MRP mutant by multicopy *CDC5*, we expected an increased temperature sensitivity in the *cdc5*/RNase MRP double mutants. This result was borne out in all four RNase MRP mutants tested (see Figure 9). The extreme case was in the *snm1-p18* mutation that could not be combined with the *cdc5-1* mutation. Taken together, RNase MRP mutants exhibit a high degree of genetic interaction with EFM mutants.

## DISCUSSION

**RNase MRP mutations and exit from mitosis:** The M-to-$G_1$ cell cycle delay in RNase MRP mutants was originally identified in the YMC6 strain that had a slow growth phenotype and displayed cells arrested with large buds, well-divided nuclei, and extended contiguous spindles. We demonstrate that temperature-sensitive mutations in both the MRP RNA component and the unique protein component (Schmitt and Clayton 1993; Cai *et al.* 1999; Shadel *et al.* 2000) have an accumulation of cells in telophase. In addition, we identified a plasmid missegregation defect that has also been reported in other EFM mutants (Hardy and Pautz 1996; Shou and Deshaies 2002). The plasmid missegregation is most likely the result of the long delay of cells in telophase (Cai *et al.* 1999). Together these results suggest that the cell cycle phenotype is due to the loss of RNase MRP function, as opposed to the loss of individual enzyme components, and that RNase MRP enzymatic activity may be an important component for EFM. In our strongest temperature-sensitive RNase MRP RNA mutant, we saw an accumulation of >70% of the cells in telophase at the nonpermissive temperature. Because we did not see all of the cells in the telophase arrest, we consider this a cell cycle delay as opposed to an arrest.

Examination of the RNase MRP RNA mutant revealed that Clb2 protein accumulates in this strain. In wild-type cells, Clb2 protein is expressed in late S phase and degrades rapidly after anaphase. Destruction of Clb2 cyclin plays an important role in cyclin-dependent kinase (Cdk) inactivation and exit from mitosis (Visintin *et al.* 1998). Elevated Clb2 protein levels are a ubiquitous characteristic of EFM mutants and excess Clb2p promotes accumulation of cells at telophase. This is also true of RNase MRP mutants and indicates that MRP mutants accumulate at a similar cell cycle stage by a similar mechanism as other EFM mutants. Furthermore, we have shown that the accumulation of Clb2p is a result of an increase in steady-state levels of *CLB2* mRNA. *CLB2* transcripts begin to accumulate late in S phase, remain elevated until late in mitosis, and are degraded rapidly as cells complete mitosis (Fitch *et al.* 1992). This suggests that *CLB2* mRNA levels play an important role in control of Clb2-CDK activity. Transcription plays a major part in the control of *CLB2* mRNA levels in the cell cycle. However, little has been reported about how *CLB2* mRNA is degraded, even though degradation of the mRNA is essential for tight control of the mRNA levels. It is noteworthy that *cdc15* mutants arrested in telophase have been reported to show very low levels of the *CLB2* mRNA (Fitch *et al.* 1992); this is in contrast to what we observe in RNase MRP mutants. On the basis of these observations it is clearly worth investigating if RNase MRP plays a role in degrading B-cyclin mRNAs.

Cdc14, a protein phosphatase and a EFM mutant, is found inactively sequestered in the nucleolus during most of the cell cycle and released in telophase to spread through the cell and dephosphorylate Swi5, Sic1, and Hct1/Cdh1. Dephosphorylation of these substrates is required to degrade the Clb2 protein and inactivate the kinase. Since RNase MRP is located in the nucleolus where it processes rRNAs (Schmitt and Clayton 1993), we examined mobilization of Cdc14. We found Cdc14 release to be normal in MRP mutants, suggesting that the regulatory mechanism of Clb2 proteolysis is also functional. Proper functioning of this pathway is also consistent with the identification of *CDC5* as a high-copy suppressor of an RNase MRP mutant.

Cdc5 is a rate-limiting determinant of APC/C activity and B-cyclin destruction. Overexpression of Cdc5 has been shown to lead to increased destruction of Clb2 protein and suppression of other EFM mutants (Shirayama *et al.* 1998). *CDC5* rescues the *snm1-172* mutation growth defect, without restoring the rRNA processing defect. This finding indicates that the cell cycle delay

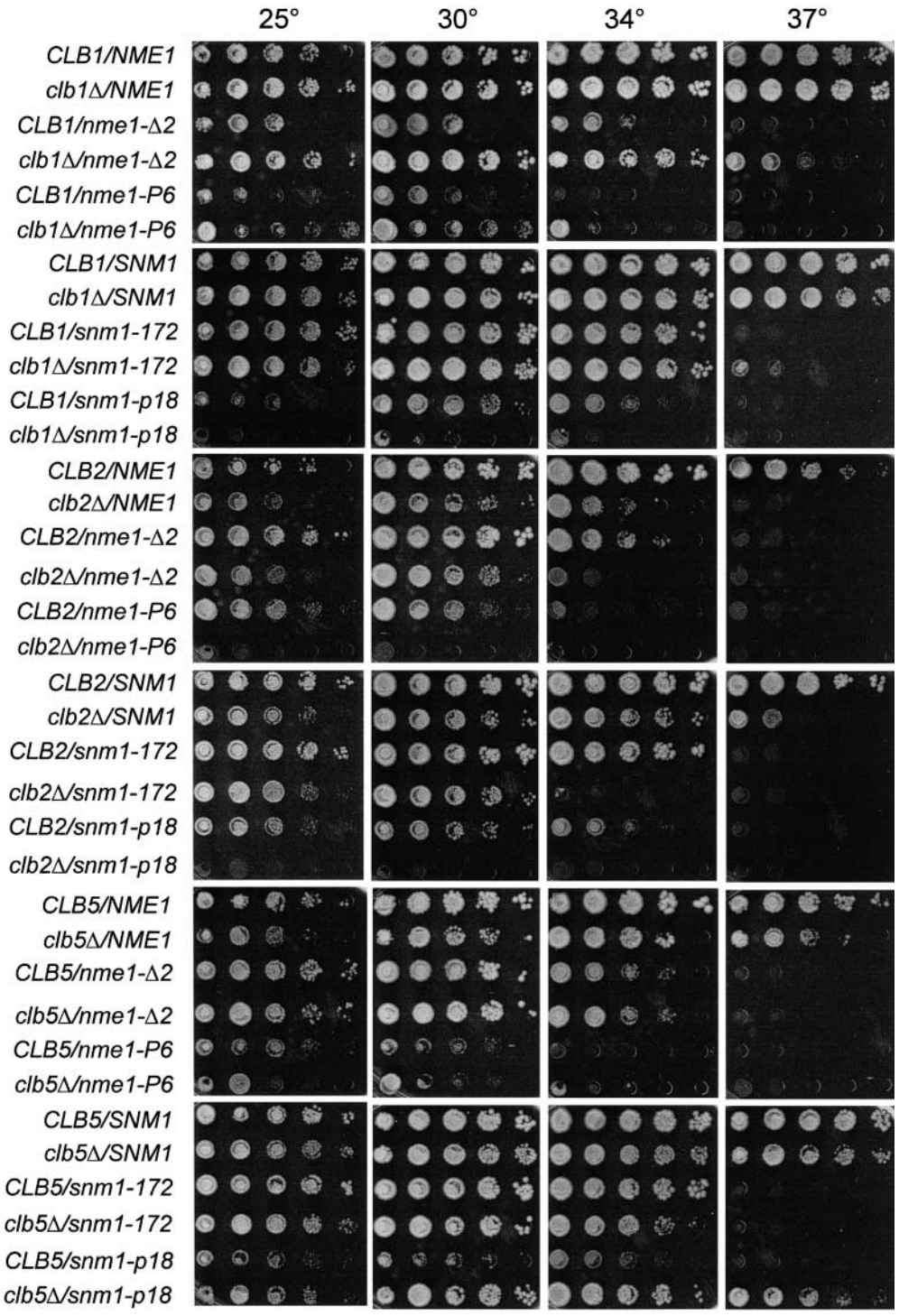


FIGURE 8.—Growth phenotypes of double RNase MRP and B-cyclin mutants. Consecutive 10-fold dilutions of each indicated strain were made in a microtiter dish, spot plated (using a 48-pin replica-plating device) onto YPD plates, and grown at the indicated temperature. The images are a composite of several plates and the experiment was repeated three times to ensure reproducibility. The full genotypes of strains are provided in Table 1.

caused by RNase MRP mutations is the result of the accumulated Clb2 cyclin and not defective rRNA processing. This is consistent with the view that rRNA processing is not the essential function of RNase MRP and an additional function is essential (HENRY *et al.* 1994; VENEMA and TOLLERVEY 1999).

We were able to identify a number of genetic interactions between RNase MRP mutations and both EFM mutations and B-cyclin deletions. On the basis of the phenotypes of these double mutants there is a clear role for RNase MRP in the pathway leading to exit from mitosis. The phenotypes of the double mutants indicate that RNase MRP is directly involved in modulating B-cyclin levels but does not place MRP in that pathway.

Cdc14p was found to be released normally from the nucleolus in a RNase MRP mutant. Since this is one of the last steps in the known mitotic exit pathway, RNase MRP must be acting at a stage downstream from this

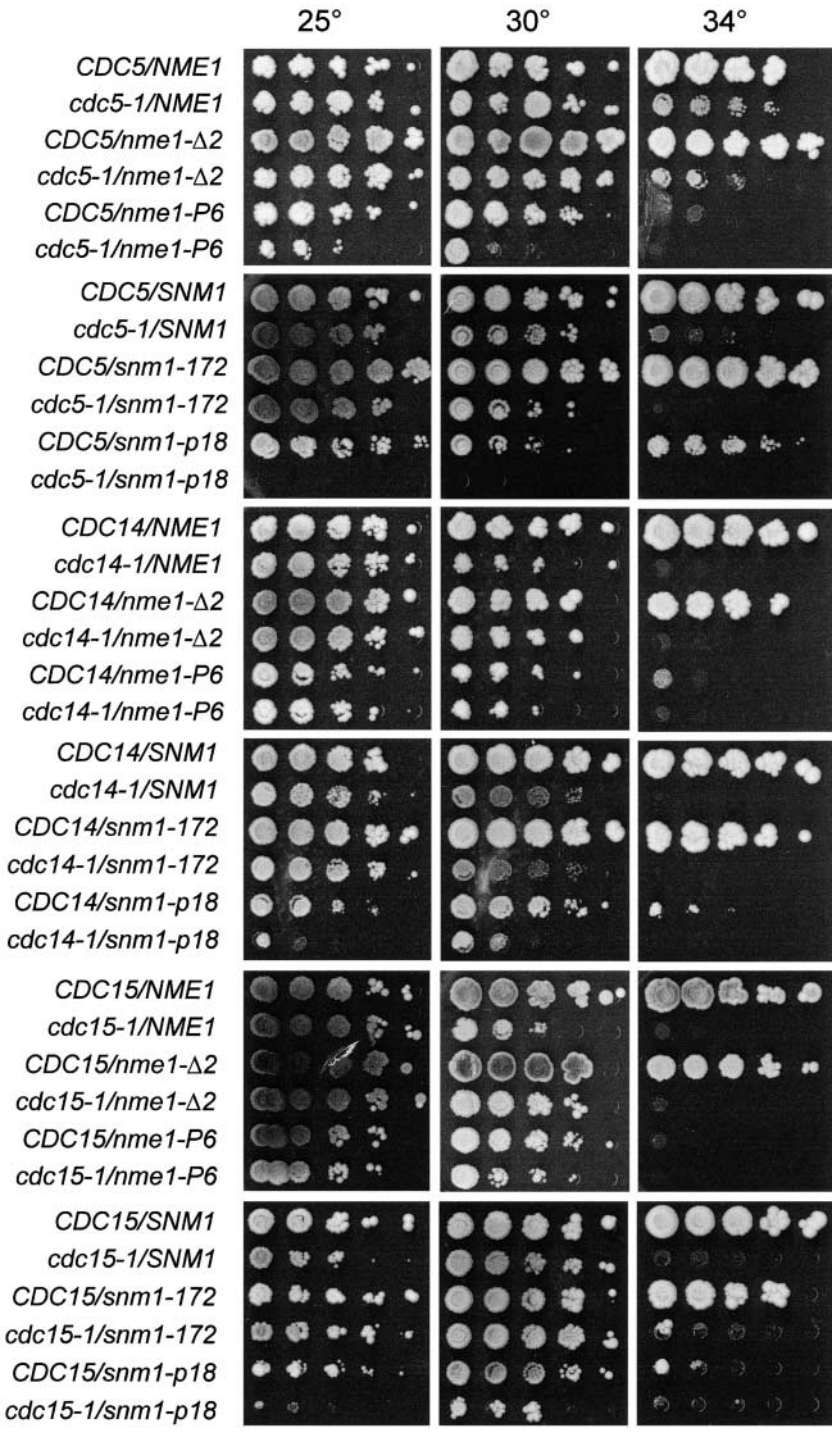


FIGURE 9.—Growth phenotypes of double RNase MRP and EFM mutants. Consecutive 10-fold dilutions of each indicated strain were made in a microtiter dish, spot plated (using a 48-pin replica-plating device) onto YPD plates, and grown at the indicated temperature. The images are a composite of several plates and the experiment was repeated three times to ensure reproducibility. The full genotypes of strains are provided in Table 1.

point or in a parallel pathway that effects B-cyclin accumulation. In *S. cerevisiae*, Clb1 and Clb2 are an important functionally redundant pair of B-type cyclins required for initiation and completion of mitosis. Clb2 is the predominant cyclin of this pair. Increased levels of Clb1/2 proteins correlate with associated CDK activity, which peaks just before and disappears immediately following anaphase. Suppression of RNase MRP mutants by the *clb1*Δ and *clb5*Δ indicates that a mild reduction in cyclin levels may be enough to pass through the MRP block. The increase in temperature sensitivity found with the RNase MRP mutants and the *clb2*Δ or the EFM mutations indicates that a drastic reduction or increase in B-cyclin levels results in an exacerbation of the MRP block.

**RNase MRP and cartilage hair hypoplasia:** Mutations in the RNA component of the human RNase MRP have been shown to cause a pleiotropic disease, cartilage hair hypoplasia (RIDANPÄÄ *et al.* 2001). This disease is manifested by short stature, sparse and brittle hair, and a compromised immune system (MÄKITIE *et al.* 1995, 1998;

Clayton 2001). The underlying problem of all of these phenotypes is a common cell proliferation defect (Pierce and Polomar 1982; Juvonen *et al.* 1995). On the basis of conservation to the yeast RNase MRP system, it is tempting to speculate that human RNase MRP is playing a similar role. We are currently investigating this possibility.

We thank M. Hale, P. Kane, and D. Amberg for comments and helpful discussions during the preparation of this manuscript. We are grateful to P. Kane, SUNY Upstate Medical University, for the Vma1 antibody and D. Amberg, SUNY Upstate Medical University, D. Hallberg, Syracuse University, D. Botstein, Stanford University, and L. Lindahl, University of Maryland Baltimore County, for strains and plasmids. This work was supported by grant no. RPG-96-109 from the American Cancer Society.

## LITERATURE CITED

Cai, T., and M. E. Schmitt, 2001 Characterization of RNase MRP function. Methods Enzymol. **342:** 135–142.

Cai, T., T. R. Reilly, M. Cerio and M. E. Schmitt, 1999 Mutagenesis of *SNM1*, which encodes a protein component of the yeast RNase MRP, reveals a role for this ribonucleoprotein endoribonuclease in plasmid segregation. Mol. Cell. Biol. **19:** 7857–7869.

Carlson, M., and D. Botstein, 1982 Two differentially regulated mRNAs with different 5′ ends encode secreted with intracellular forms of yeast invertase. Cell **28:** 145–154.

Chamberlain, J. R., Y. Lee, W. S. Lane and D. R. Engelke, 1998 Purification and characterization of the nuclear RNase P holoenzyme complex reveals extensive subunit overlap with RNase MRP. Genes Dev. **12:** 1678–1690.

Chang, D. D., and D. A. Clayton, 1987 A novel endoribonuclease cleaves at a priming site of mouse mitochondrial DNA replication. EMBO J. **6:** 409–417.

Charles, J. F., S. L. Jaspersen, R. L. Tinker-Kulberg, L. Hwang, A. Szidon *et al.*, 1998 The Polo-related kinase Cdc5 activates and is destroyed by the mitotic cyclin destruction machinery in *S. cerevisiae*. Curr. Biol. **8:** 497–507.

Chu, S., R. H. Archer, J. M. Zengel and L. Lindahl, 1994 The RNA of RNase MRP is required for normal processing of ribosomal RNA. Proc. Natl. Acad. Sci. USA **2:** 659–663.

Chu, S., J. M. Zengel and L. Lindahl, 1997 A novel protein shared by RNase MRP and RNase P. RNA **3:** 382–391.

Clayton, D. A., 2001 A big development for a small RNA. Nature **410:** 29–31.

Cross, F. R., V. Archambault, M. Miller and M. Klovstad, 2002 Testing a mathematical model of the yeast cell cycle. Mol. Biol. Cell **13:** 52–70.

Dichtl, B., and D. Tollervey, 1997 Pop3p is essential for the activity of the RNase MRP and RNase P ribonucleoproteins in vivo. EMBO J. **16:** 417–429.

Fitch, I., C. Dahmann, U. Surana, A. Amon, K. Nasmyth *et al.*, 1992 Characterization of four B-type cyclin genes of the budding yeast *Saccharomyces cerevisiae*. Mol. Biol. Cell **3:** 805–818.

Hardy, C. F., and A. Pautz, 1996 A novel role for Cdc5p in DNA replication. Mol. Cell. Biol. **16:** 6775–6782.

Hartwell, L. H., J. Culotti, J. R. Pringle and B. J. Reid, 1974 Genetic control of the cell division cycle in yeast. Science **183:** 46–51.

Henry, Y., H. Wood, J. P. Morrissey, E. Petfalski, S. Kearsey *et al.*, 1994 The 5′ end of yeast 5.8S rRNA is generated by exonucleases from an upstream cleavage site. EMBO J. **13:** 2452–2463.

Jaspersen, S. L., J. F. Charles, R. L. Tinker-Kulberd and D. O. Morgan, 1998 A late mitotic regulatory network controlling cyclin destruction in *Saccharomyces cerevisiae*. Mol. Biol. Cell **9:** 2803–2817.

Juvonen, E., O. Mäkitie, A. Mäkipernaa, T. Ruutu, I. Kaitila *et al.*, 1995 Defective in-vitro colony formation of haematopoietic progenitors in patients with cartilage-hair hypoplasia and history of anemia. Eur. J. Pediatr. **154:** 30–34.

Kitada, K., A. L. Johnson, L. H. Johnston and A. Sugino, 1993 A multicopy suppressor gene of the *Saccharomyces cerevisiae* $G_1$ cell cycle mutant gene *dbf4* encodes a protein kinase and is identified as *CDC5*. Mol. Cell. Biol. **13:** 4445–4457.

Longtine, M. S., A. McKenzie, D. J. Demarini, N. G. Shah, A. Wach *et al.*, 1998 Additional modules for versatile and economical PCR-based gene deletion and modification in *Saccharomyces cerevisiae*. Yeast **14:** 953–961.

Lygerou, Z., P. Mitchell, E. Petfalski, B. Séraphin and D. Tollervey, 1994 The *POP1* gene encodes a protein component common to the RNase MRP and RNase P ribonucleoproteins. Genes Dev. **8:** 1423–1433.

Lygerou, Z., H. Pluk, W. J. van Venrooij and B. Seraphin, 1996 hPop1: an autoantigenic protein subunit shared by the human RNase P and RNase MRP ribonucleoproteins. EMBO J. **15:** 5936–5948.

Mäkitie, O., T. Sulisalo, A. de la Chapelle and I. Kaitila, 1995 Cartilage-hair hypoplasia. Med. Genet. **32:** 39–43.

Mäkitie, O., I. Kaitila and E. Savilahti, 1998 Susceptibility to infections and *in vitro* immune functions in cartilage-hair hypoplasia. Eur. J. Pediatr. **157:** 816–820.

Paluh, J. L., and D. A. Clayton, 1996 A functional dominant mutation in *Schizosaccharomyces pombe* RNase MRP RNA affects nuclear RNA processing and requires the mitochondrial-associated nuclear mutation *ptp1-1* for viability. EMBO J. **15:** 4723–4733.

Pierce, G. F., and S. H. Polomar, 1982 Lymphocyte dysfunction in cartilage hair hypoplasia. II. Evidence for a cell cycle specific defect in T cell growth. Clin. Exp. Immunol. **50:** 621–628.

Pringle, J. R., A. E. Adams, D. G. Drubin and B. K. Haarer, 1991 Immunofluorescence methods for yeast. Methods Enzymol. **194:** 565–602.

Reimer, G., I. Raska, U. Scheer and E. M. Tan, 1988 Immunolocalization of 7–2-ribonucleoprotein in the granular component of the nucleolus. Exp. Cell Res. **176:** 117–128.

Ridanpää, M., H. van Eenennaam, K. Pelin, R. Chadwick, C. Johnson *et al.*, 2001 Mutations in the RNA component of RNase MRP cause a pleiotropic human disease, cartilage-hair hypoplasia. Cell **104:** 195–203.

Sambrook, J., E. F. Fritsch and T. Maniatis, 1989 *Molecular Cloning: A Laboratory Manual*. Cold Spring Harbor Laboratory Press, Cold Spring Harbor, NY.

Schmitt, M. E., and D. A. Clayton, 1992 Yeast site-specific ribonucleoprotein endoribonuclease MRP contains an RNA component homologous to mammalian RNase MRP RNA and essential for cell viability. Genes Dev. **6:** 1975–1985.

Schmitt, M. E., and D. A. Clayton, 1993 Nuclear RNase MRP is required for correct processing of pre-5.8S rRNA in *Saccharomyces cerevisiae*. Mol. Cell. Biol. **13:** 7935–7941.

Schmitt, M. E., and D. A. Clayton, 1994 Characterization of a unique protein component of yeast RNase MRP: an RNA-binding protein with a zinc-cluster domain. Genes Dev. **8:** 2617–2628.

Schmitt, M. E., T. A. Brown and B. L. Trumpower, 1990 A rapid and simple method for preparation of RNA from *Saccharomyces cerevisiae*. Nucleic Acids Res. **18:** 3091–3092.

Shadel, G. S., G. A. Buckenmeyer, D. A. Clayton and M. E. Schmitt, 2000 Mutational analysis of the RNA component of *Saccharomyces cerevisiae* RNase MRP reveals distinct nuclear phenotypes. Gene **245:** 175–184.

Shirayama, M., W. Zachariae, R. Ciosk and K. Nasmyth, 1998 The Polo-like kinase Cdc5p and the WD-repeat protein Cdc20p/fizzy are regulators and substrates of the anaphase promoting complex in *Saccharomyces cerevisiae*. EMBO J. **17:** 1336–1349.

Shortle, D., J. E. Haber and D. Botstein, 1982 Lethal disruption of the yeast actin gene by integrative DNA transformation. Science **217:** 371–373.

Shou, W., and R. J. Deshaies, 2002 Multiple telophase arrest bypassed (*tab*) mutants alleviate the essential requirement for Cdc15 in exit from mitosis in *S. cerevisiae*. BMC Genet. **3:** 4.

Shou, W., J. H. Seol, A. Shevchenko, C. Baskerville, D. Moazed *et al.*, 1999 Exit from mitosis is triggered by Tem1-dependent release of the protein phosphatase Cdc14 from nucleolar RENT complex. Cell **97:** 233–244.

Shu, Y., H. Yang, E. Hallberg and R. Hallberg, 1997 Molecular genetic analysis of Rts1p, a B′ regulatory subunit of *Saccharomyces cerevisiae* protein phosphatase 2A. Mol. Cell. Biol. **17:** 3242–3253.

Sikorski, R. S., and J. D. Boeke, 1991 In vitro mutagenesis and

plasmid shuffling: from cloned gene to mutant yeast. Methods Enzymol. **194:** 302–318.

Spellman, P. T., G. Sherlock, M. Q. Zhang, V. R. Iyer, K. Anders *et al.*, 1998 Comprehensive identification of cell cycle-regulated genes of the yeast *Saccharomyces cerevisiae* by microarray hybridization. Mol. Biol. Cell **9:** 3273–3297.

Stolc, V., and S. Altman, 1997 Rpp1, an essential protein subunit of nuclear RNase P required for processing of precursor tRNA and 35S precursor rRNA in *Saccharomyces cerevisiae*. Genes Dev. **11:** 2414–2425.

Surana, U., A. Amon, C. Dowzer, J. McGrew, B. Byers *et al.*, 1993 Destruction of the CDC28/CLB mitotic kinase is not required for the metaphase to anaphase transition in budding yeast. EMBO J. **12:** 1969–1978.

van Eenennaam, H., N. Jarrous, W. J. van Venrooij and G. J. Pruijn, 2000 Architecture and function of the human endonucleases RNase P and RNase MRP. IUBMB Life **49:** 265.

Venema, J., and D. Tollervey, 1999 Ribosome synthesis in *Saccharomyces cerevisiae*. Annu. Rev. Genet. **33:** 261–311.

Visintin, R., K. Craig, E. S. Hwang, S. Prinz, M. Tyers *et al.*, 1998 The phosphatase Cdc14 triggers mitotic exit by reversal of Cdk-dependent phosphorylation. Mol. Cell **2:** 709–718.

Visintin, R., E. S. Hwang and A. Amon, 1999 Cfi1 prevents premature exit from mitosis by anchoring Cdc14 phosphatase in the nucleolus. Nature **398:** 818–823.

Zachariae, W., and K. Nasmyth, 1999 Whose end is destruction: cell division and the anaphase-promoting complex. Genes Dev. **13:** 2039–2058.

Communicating editor: S. Sandmeyer